# Destruction of the Global Phase Coherence in Ultrathin, Doubly Connected Superconducting Cylinders

Y. Liu,* Yu. Zadorozhny, M. M. Rosario, B. Y. Rock, P. T. Carrigan, H. Wang

**In doubly connected superconductors, such as hollow cylinders, the fluxoid is known to be quantized, allowing the superfluid velocity to be controlled by an applied magnetic flux and the sample size. The sample-size–induced increase in superfluid velocity has been predicted to lead to the destruction of superconductivity around half-integer flux quanta. We report transport measurements in ultrathin Al and $Au_{0.7}In_{0.3}$ cylinders verifying the presence of this destructive regime characterized by the loss of the global phase coherence and reveal a phase diagram featuring disconnected phase coherent regions, as opposed to the single region seen in larger superconducting cylinders studied previously.**

Recent advances in nanoscience have demonstrated that fundamentally new physical phenomena may be found when the size of samples shrinks. In the area of superconductivity, the reduction of sample size has led to the observation of the paramagnetic Meissner effect in micrometer-size superconductors (*1*), the quantization of the Bose condensate in submicrometer samples (*2*), and ultimately the suppression of superconductivity in nanometer-scale superconductors (*3*, *4*). In this regime, it has also been recognized that the sample topology has particularly strong effects on superconductivity (*5*), as reflected in the characteristic features of the phase diagrams for a filled square and a loop (*6*). The same result is expected for any samples of singly and doubly connected geometry, topological terms for objects free of or possessing a hole, respectively.

In the mixed state, a magnetic field can penetrate the interior of a superconductor in quantized vortex lines, with supercurrents circulating around the vortex core. One feature of doubly connected superconductors (independent of the sample size) is that the circulating Cooper pairs lead to the quantization of the fluxoid (*7*, *8*), rather than the vortex, in units of $\Phi_0 = h/2e$ (in SI units), where $h$ is the Planck constant and $e$ is the electron charge, because of the presence of global phase coherence among the Cooper pairs (*9*). Global phase coherence, whose presence is indicated by a zero resistance state, refers to the fact that a macroscopic wave function can be used to describe the motion of all Cooper pairs in a superconducting sample. The fluxoid, $\Phi'$, is defined by

$$\Phi' = \Phi + (m^*c/e^*)\oint_C v_s \cdot ds \qquad (1)$$

where $\Phi = \int \mathbf{H} \cdot d\mathbf{S} = \oint_C \mathbf{A} \cdot d\mathbf{s}$ is the ordinary magnetic flux, $m^*$ and $e^*$ are the effective mass and charge of the Cooper pairs, respectively, $v_s$ is the tangential superfluid velocity, and $C$ is a closed contour in the superconductor. If $C$ is deep in a (bulk) superconductor, $v_s$ vanishes so that $\Phi' \approx \Phi$.

For a cylinder with an insulating or hollow core, if the wall thickness is smaller than the superconducting penetration depth, then $v_s$ is uniform in the sample (*10*). In this case, because of fluxoid quantization, for a given flux $\Phi$,

$$v_s=(2\hbar/m^*d)(n-\Phi/\Phi_0) \qquad (2)$$

where $\hbar = h/2\pi$, $d$ is the cylinder diameter, and $n$ is an integer that minimizes $v_s$, leading to the Little-Parks effect (*11*), characterized by a small oscillation in $v_s$ that results in an oscillation in the superconducting transition temperature ($T_c$) and the sample resistance in the transition regime, with a period of $\Phi_0$.

It was pointed out that a consequence of fluxoid quantization in ultrasmall superconductors, within the phenomenological Ginzburg-Landau theory, was that for a superconducting ring with a side arm of length $L$ and diameter $d$, two very different physical regimes should emerge for different ring diameters (*5*). For large rings, the conventional Little-Parks effect, with a small oscillation in $T_c$, should be found, and superconductivity should exist at zero temperature in all magnetic fields up to the critical field. However, for $d < \xi(0)$, where $\xi(0)$ is the zero temperature superconducting coherence length, a destructive regime should occur. For a simple ring with $L = 0$, the solution of the Ginzburg-Landau equation leads to (*5*, *12*)

$$\cos\left(2\pi\,\frac{\Phi}{\Phi_0}\right) = \cos\left(2\pi\,\frac{d/2}{\xi(T)}\right) \qquad (3)$$

where $\xi(T) = \xi(0)[T_c/(T_c - T)]^{1/2}$. Therefore, when $d < \xi(0)$, for $\Phi$ given by

$$(k\Phi_0 - \Delta\Phi)/2 < \Phi < (k\Phi_0 + \Delta\Phi)/2 \quad (4)$$

where $k$ is an odd integer and $\Delta\Phi = [1 - d/\xi(0)]\Phi_0$, Eq. 3 does not have a solution, making superconductivity not possible even at $T = 0$. The superconducting-normal (S-N) phase boundary, derived from Eq. 3, is given by

$$\left(n - \frac{\Phi}{\Phi_0}\right)^2 = \left(\frac{d/2}{\xi(0)}\right)^2\left(1 - \frac{T}{T_c}\right) \quad (5)$$

This destruction of superconductivity at zero temperature is directly related to the sample-size–induced increase in $v_s$ in a doubly connected superconductor. Within the Ginzburg-Landau free energy, the kinetic energy density of the supercurrent, $1/2n_s^*m^*v_s^2$ (where $n_s^*$ is the number density of the Cooper pairs), can be compared with the superconducting condensation energy density in an applied field, $H_c^2/8\pi + H^2/8\pi = n_s^*\,\hbar^2/4m^*\xi^2(T) + H^2/8\pi$ (where $H_c$ is the thermodynamic critical field and $H$ is the applied field). Equation 2 suggests that the doubly connected sample geometry demands that $v_s$ increase toward its maximum value of $v_s^{max} = \hbar/m^*d$ at half-integer flux quanta, as long as global phase coherence is present in the sample. Qualitatively, if $d$ is made sufficiently small, the kinetic energy would be pushed so high (as the flux nears half-integer quanta) that it would be impossible to compensate this energy by the condensation energy, making the globally phase coherent superconducting state energetically unfavorable. This particular way of suppressing superconductivity is fundamentally different from that by strong disorder or Coulomb repulsion (*13*).

Experimentally, this phenomenon is difficult to observe. If rings, prepared by e-beam lithography, are used, the condition $d < \xi(0)$ requires the rings to be extremely small in diameter and, therefore, linewidth. These types of samples typically have short coherence lengths, because of the unavoidable disorder introduced by structural defects and boundary roughness. For example, $\xi(0)$ was found to be only 0.1 to 0.2 μm in mesoscopic Al disks, squares, and loops (*2*, *6*). In comparison, $\xi(0)$ should be 1.6 μm in single crystalline Al (*14*). In (*6*), the effect of sample geometry on mesoscopic superconductors was experimentally studied. Indeed, the phase diagram for a singly connected sample was found to be substantially different from that of a doubly connected loop of the same size because of the absence of orbital (vortex) states in the latter type of samples. However, the sizes of the samples in this previous study [1 μm, an order of magnitude larger than $\xi(0) = 0.1$ μm] were too large to reach the regime considered theoretically. Ultrathin cylinders, which have advantages over the rings for detecting the de-

Department of Physics, The Pennsylvania State University, University Park, PA 16802, USA.

*To whom correspondence should be addressed. E-mail: liu@phys.psu.edu

structive regime because these samples can have high parallel critical fields and reasonably long superconducting coherence lengths, were chosen for the present study.

The cylindrical samples (Fig. 1B) were prepared by depositing Al or $Au_{0.7}In_{0.3}$ onto an insulating quartz filament, as previously described (*15*, *16*). The cylinders were ≤1 mm long and as small as 150 nm in diameter, nearly an order of magnitude smaller than previously studied (*7*). Electrical transport measurements were carried out in a dilution or a $^3$He refrigerator equipped with a superconducting magnet, with base temperatures of 20 mK and 0.3 K, respectively. The cylinders were manually aligned to be parallel to the magnetic field. The cylinder diameters were inferred from the resistance oscillation period and confirmed by atomic force microscope measurements.

The resistance of an Al cylinder (Al-1, $d$ = 150 nm) is plotted as a function of $\Phi$ and $T$ (Fig. 1A), where it is seen that at low $T$, the sample was superconducting for a substantial range of magnetic field below $H_{c//}$. However, the zero sample resistance was suppressed around $\Phi = \pm 1/2\Phi_0$ and $\pm 3/2\Phi_0$, resulting in narrow resistance peaks. At the lowest temperature, $T$ = 20 mK, the resistance peaks at $\Phi = \pm 1/2\Phi_0$ had a magnitude $R \approx 310$ ohms, a substantial fraction of the normal-state resistance $R_N \approx 930$ ohms, and a width of about $0.18\Phi_0$, as measured at the onset of nonzero resistance.

The temperature dependence of the sample resistance measured in zero and finite fields corresponding to integer and half-integer flux quanta (Fig. 2A) shows that, at zero field, Al-1 became superconducting around 1.3 K. At $1/2\Phi_0$, its resistance showed a broad drop starting around 1 K, in strong contrast with $R(T)$ at $\Phi = \Phi_0$, where a sharp transition to zero resistance was seen at 1 K even though the applied field was higher. Similar behavior was also observed in an ultrathin cylinder of $Au_{0.7}In_{0.3}$ (AuIn-1, $d$ = 154 nm) (Fig. 2B). For both Al-1 and AuIn-1, $R(T)$ at $1/2\Phi_0$ leveled off to a substantial fraction of $R_N$, showing almost no change from 200 mK down to 20 mK. In contrast, the temperature dependence of a larger Al cylinder (Al-2, $d$ = 357 nm) (Fig. 3) displayed a conventional $T_c$ oscillation with no essential difference in the shape of $R(T)$ at integer and half-integer flux quanta.

The systematic behavior observed in all samples suggests that a sample with a sufficiently small diameter may remain nonsuperconducting around half-integer flux quanta even at zero temperature. A generic phase diagram can thus be obtained for ultrasmall, doubly connected superconducting samples (Fig. 4), where a normal phase extends deep into the region where superconductivity would be expected for cylinders of a conventional size. For these samples, the well-established phase diagram consists of a single superconducting region with a slightly modulated phase boundary extending up to the parallel critical field, $H_{c//}$ (Fig. 3, inset B). This new phase diagram is qualitatively different, featuring disconnected phase coherent regions separated by a resistive phase.

To compare our experimental results with the theory, it is useful to determine $\xi(0)$. Finite-temperature $\xi(T)$ can be estimated from $H_{c//}(T) = \sqrt{3}\,\Phi_0/\pi t\xi(T)$, where $t$ is the film thickness (*17*). Using the onset $H_{c//}(T)$, values of $\xi(T)$ are found to be 161 nm for Al-1 ($d$ = 150 nm) at 20 mK, 160 nm for AuIn-1 ($d$ = 154 nm) at 20 mK, and 60 nm for Al-2 ($d$ = 357 nm) at 0.39 K [$\xi(0) < 60$ nm]. Therefore, we may conclude that $d < \xi(0)$ for both Al-1 and AuIn-1, whereas $d > \xi(0)$ for Al-2 (which is more disordered than Al-1), as expected theoretically.

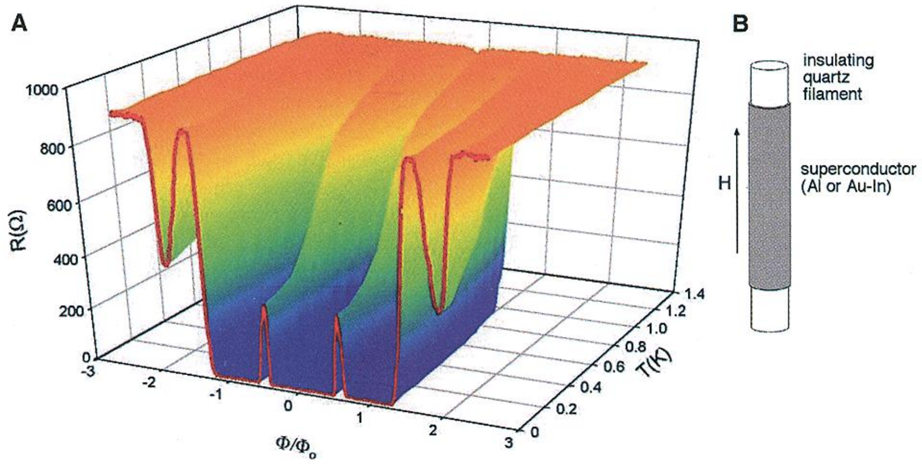


**Fig. 1.** **(A)** Resistance as a function of $\Phi$ and $T$ for Al-1, an Al cylinder with diameter $d$ = 150 nm and wall thickness $t$ = 30 nm. Even at temperatures much lower than the zero-field $T_c$ (=1.30 K at onset), the sample remained normal around $\Phi = \pm 1/2\Phi_0$ and $\pm 3/2\Phi_0$. At $T$ = 20 mK, the resistance peak at $\Phi = \pm 1/2\Phi_0$ has a width of $\Delta\Phi = 0.18\Phi_0$ and a magnitude of $R = 0.33R_N$, where $R_N$ (= 930 ohms) is the normal-state resistance. The superconducting coherence length $\xi$(20 mK) is about 161 nm, as estimated from the parallel critical field $H_{c//}$(20 mK) = 2365 G ($\Phi_c = 2.03\Phi_0$). Values of resistance were taken every $0.01\Phi_0$ from $-2.5\Phi_0$ to $+2.5\Phi_0$, at 20 mK and every 100 mK starting from 0.10 K up to 1.30 K. The solid red line connects the data points taken at 20 mK. **(B)** Schematic of the sample configuration.

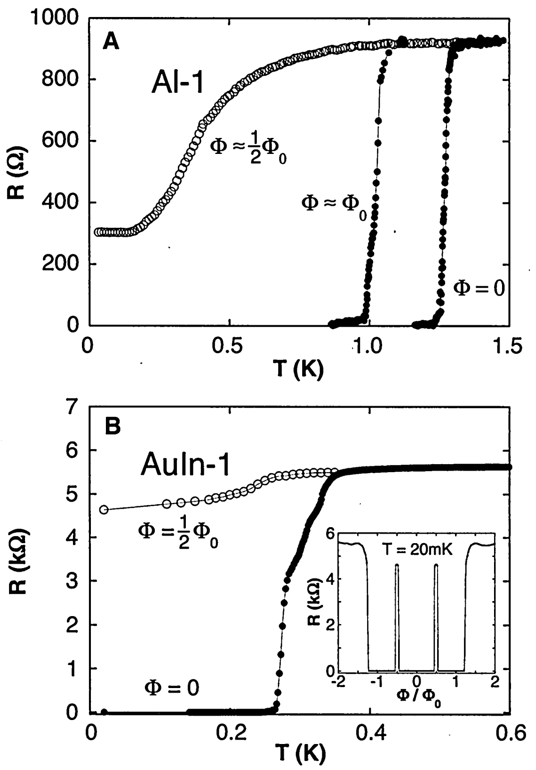


**Fig. 2.** **(A)** Resistance versus temperature at several values of magnetic flux for Al-1. Filled and open circles correspond to resistances taken at integer and half-integer flux quanta, respectively. Whereas sharp transitions to zero resistance were observed at integer $\Phi_0$, a broad drop characterized the behavior at $1/2\Phi_0$, where the resistance leveled off to a substantial fraction of the normal-state resistance at temperatures below 200 mK. Lines are used to connect the data points. **(B)** Resistance versus temperature at several values of magnetic flux for AuIn-1, a $Au_{0.7}In_{0.3}$ cylinder with $d$ = 154 nm and $t$ = 30 nm. Filled and open circles correspond to resistances taken at integer and half-integer flux quanta, respectively. The resistance at $1/2\Phi_0$ leveled off to about $0.80R_N$ ($R_N$ = 5.64 kiloohms), showing almost no change from 200 mK down to 20 mK. Lines are used to connect the data points. **(Inset)** $R(\Phi)$ for AuIn-1 at $T$ = 20 mK. For most fields below $H_{c//}$ the sample was superconducting, except around $\Phi = \pm 1/2\Phi_0$, where sharp resistance peaks of width $\Delta\Phi = 0.1\ \Phi_0$ were found. From $H_{c//}$ = 2382 G ($\Phi_c = 2.14\Phi_0$), $\xi$(20 mK) is estimated to be 160 nm.

To fit the experimentally obtained S-N phase boundary requires taking into account several effects not explicitly considered in the theory presented in (*5*). For example, any misalignment of the cylinder axis with the magnetic field would result in a diamagnetic response that leads to a parabolic envelope of the S-N phase boundary (*10*). In addition, the effects of finite wall thickness, and the suppression of the amplitude of the superconducting order parameter by the applied parallel field, become increasingly important in ultrathin cylinders (*10*). A fit to Eq. 5 is attempted by assigning a different value of $T_c$ to the $n = 0$ and $n = 1$ region of the phase boundary without considering these effects in detail, resulting in a surprisingly good fit (Fig. 4) despite the simplification.

Several questions of fundamental interest are raised by these results. A substantial drop in $R(T)$ taken at half-integer flux quanta was found in Al-1 and, to a lesser extent, in AuIn-1. The origin of the resistance drop should be related to superconductivity. As discussed above, the zero temperature finite-resistance state observed in the destructive regime only indicates the loss of global phase coherence. It might be reasonable to ask whether the local pair formation may have survived, thereby leading to a novel resistive phase of Cooper pairs.

It is possible that a finite-resistance state can arise from a dynamical switching of the fluxoid number in ultrathin cylinders. Switching between $n = 0$ and $n = 1$ states around $\Phi = \Phi_0/2$, for example, requires vortex motion through the cylinder wall, leading to a finite resistance, a scenario analogous to the finite resistance caused by phase slips in one-dimensional superconducting wires (*17*). It should be noted, however, that the loss of the global phase coherence in this system occurs even at $T = 0$. Therefore, quantum phase slips (*18*) would have to be considered to account for the observed resistive state in the current experiment. Alternatively, this may be related to the resistive state proposed for superconductors coupled to a dissipative bath (*19*). More experiments are needed to clarify the nature of the zero temperature resistive state found in the present experiment.

What would happen if the diameter of the cylinder were to be made even smaller? In particular, what should we expect when the circumference becomes smaller than the superconducting coherence length? In this limit, a Ginzburg-Landau equation in a coordinate along the circumference of the cylinder, as used in (*5*), is presumably invalid. A microscopic theory has not been attempted. Experimentally, the preparation of doubly connected superconducting samples of dimensions on the nanometer scale challenges the existing technologies. In this regard, superconducting carbon nanotubes (*20*) are a promising candidate for such studies.

Singly connected superconducting Al disks, in which global phase coherence was observed directly in samples of size smaller than $\xi(0)$ (*2*), have been studied experimentally (*1*, *2*, *6*) and theoretically (*21*, *22*). However, phenomena in singly connected superconducting wires in a parallel magnetic field, in particular those associated with vortex states (*21*, *22*), are yet to be explored. Further experiments on these nanoscale superconductors, with or without a doubly connected sample geometry, are clearly desired.

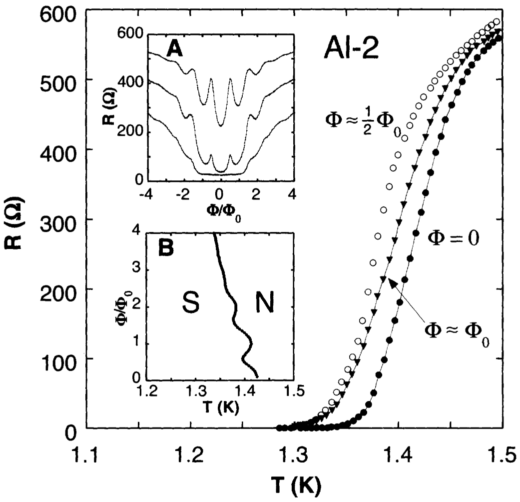


**Fig. 3.** Resistance versus temperature at several values of magnetic flux for Al-2, an Al cylinder with $d = 357$ nm and $t = 30$ nm. $\xi(T)$ is 60 nm at $T = 0.39$ K, as estimated from $H_{c//}$. Therefore, at $T = 0$, $\xi(0) < 60$ nm, and $d > \xi(0)$. **(Inset A)** $R(\Phi)$ at several temperatures. Conventional Little-Parks resistance oscillations of period $\Phi_0 = h/2e$ were present. **(Inset B)** Measured $\Phi$-$T$ phase diagram for Al-2. A single superconducting region (S), with a phase boundary modulated by an oscillation of period $\Phi_0 = h/2e$, was observed. A resistance value of $R = 400$ ohms was used to determine the superconducting-normal (S-N) phase boundary, $T_c(\Phi)$.

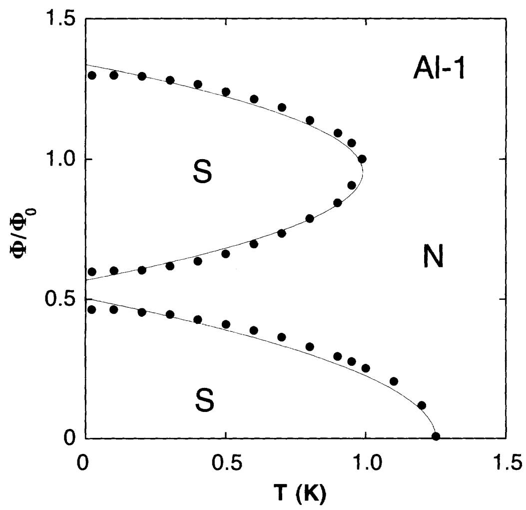


**Fig. 4.** $\Phi$-$T$ phase diagram for Al-1 ($d = 150$ nm). Disconnected superconducting regions (S) separated by a normal resistive phase (N) are found in the zero temperature limit. The solid lines are fits to theory (see text). A value of $R(T_c) = 0.05R_N$ was chosen to determine the phase boundary, $T_c(\Phi)$. The temperature range (0 to 1.5 K) is much larger than that shown for Al-2 (1.25 to 1.45 K).

**References and Notes**

1. A. K. Geim *et al.*, *Nature* **396**, 144 (1998).
2. A. K. Geim, S. V. Dabonos, J. G. S. Lok, M. Henini, J. C. Maan, *Nature* **390**, 259 (1997).
3. P. W. Anderson, *J. Phys. Chem. Solids* **11**, 26 (1959).
4. For a recent review, see M. Tinkham, D. C. Ralph, C. T. Black, J. M. Hergenrother, *Czech. J. Phys.* **46**, 3139 (1996).
5. P.-G. de Gennes, *C. R. Acad. Sci. Paris* **292**, 279 (1981).
6. V. V. Moshchalkov *et al.*, *Nature* **373**, 319 (1995).
7. B. S. Deaver Jr., W. M. Fairbank, *Phys. Rev. Lett.* **7**, 43 (1961).
8. R. Doll, M. Näbauer, *Phys. Rev. Lett.* **7**, 51 (1961).
9. C. N. Yang, *Rev. Mod. Phys.* **34**, 694 (1962).
10. P.-G. de Gennes, *Superconductivity of Metals and Alloys* (Benjamin, New York, 1966), pp. 185, 188, 189.
11. W. A. Little, R. D. Parks, *Phys. Rev. Lett.* **9**, 9 (1962).
12. J. P. Straley, P. B. Visscher, *Phys. Rev. B* **26**, 4922 (1982).
13. For a recent review, see A. M. Goldman, N. Markovic, *Phys. Today* **51**, 39 (1998).
14. C. Kittel, *Introduction to Solid State Physics* (Wiley, New York, ed. 7, 1996), p. 253.
15. Yu. Zadorozhny, D. R. Herman, Y. Liu, *Phys. Rev. B* **63**, 144521 (2001).
16. Yu. Zadorozhny, Y. Liu, *Europhys. Lett.* **55**, 712 (2001).
17. M. Tinkham, *Introduction to Superconductivity* (McGraw Hill, New York, ed. 2, 1996), pp. 119, 131, 288–293.
18. N. Giordano, *Phys. Rev. Lett.* **61**, 2137 (1988).
19. A. Kapitulnik, N. Mason, S. A. Kivelson, S. Chakravarti, *Phys. Rev. B* **63**, 125322 (2001).
20. Z. K. Tang *et al.*, *Science* **292**, 2462 (2001).
21. See, for example, P. Singha Deo, V. A. Schweigert, F. M. Peeters, A. K. Geim, *Phys. Rev. Lett.* **79**, 4653 (1997), and references therein.
22. M. B. Sobnack, F. V. Kusmartsev, *Phys. Rev. Lett.* **86**, 716 (2001), and references therein.
23. We thank A. M. Goldman, J. Jain, and J. Banavar for useful discussions; S. Diaz for translating (*5*) into English; and K. D. Nelson, Z. Q. Mao, E. Hutchinson, and D. Okuno for technical assistance. This work is supported by grants from the U.S. NSF and the Pennsylvania State University Materials Research Science and Engineering Center.

10 September 2001; 7 November 2001